HYDROGEN ABSORPTION IN A-$Co_{30}Fe_{55}B_{15}$

ČERMÁK Jiří [1,2], KRÁL Lubomír[1], ROUPCOVÁ Pavla[1,3]

[1]Institute of Physics of Materials AS CR, v.v.i., Brno, Czech Republic, EU
[2]CEITEC IPM, Institute of Physics of Materials, AS CR, Brno, Czech Republic, EU
[3] Brno University of Technology, FME, IMSE, Brno, Czech Republic, EU

Abstract

Hydrogen solved in amorphous alloys (AAs) influences their magnetic characteristics. AAs are also perspective as additives that can improve hydrogen storage kinetic in certain types of ball-milled hydrogen storage materials (HSMs). Therefore, knowledge of hydrogen solubility and hydrogen sorption kinetics in AAs are of a great importance for aimed design both AAs with optimal magnetic parameters and HSMs with desired sorption characteristics. In the present paper, amorphous alloy $Co_{30}Fe_{55}B_{15}$ (an example of the type a-$TM1_xTM2_yB_z$; TM - transition metal) was investigated. Hydrogen concentration c_H was measured by Sieverts method in temperature interval from $T = 150$ °C to $T = 350$ °C under hydrogen pressure p up to 6 MPa. It was found that c_H was an increasing function of p and its maximum value was typically 0.5 wt.% H_2 at 350 °C and 6 MPa. However, when the alloy was preliminary hydrogen charged (PHC), the pressure dependence of total c_H^{tot} in the first absorption cycle(s) is non-monotonous in dependence on PHC conditions. For the sake of comparison, the same absorption characteristics were measured also in Mg_2Ni intermetallic that is a common constituent in Mg-based HSMs. Comparing $Co_{30}Fe_{55}B_{15}$ and Mg_2Ni, it was concluded that $Co_{30}Fe_{55}B_{15}$ shows lower hydrogen solubility, but much better absorption kinetics.

Keywords: Hydrogen, absorption, $Co_{30}Fe_{55}B_{15}$

1. INTRODUCTION

Amorphous alloys (AAs) of CoFeB type have been exploited before all in the field of data recording, or as magnetic sensors because of their excellent electric and magnetic characteristics [1]. Their crystallization characteristics and thermal stability were studied, eg. in [1-5]. It appeared that some of key parameters of AAs, such as Curie temperature, electrical resistance, glass transition and crystallization temperatures etc. depend on the presence of hydrogen in the ambient environment [6, 7]. Studies that reported the relation between the electro-magnetic parameters and/or the thermal stability of melt-spun alloys on one hand and hydrogen content in the AA on the other (e.g., [8]), invoked an idea that the AAs could be consider also as a kind of hydrogen storage (HS) material.

In Ref. [8], the HS properties of Mg-based melt-spun alloys containing La and Ni were investigated. Magnesium hydride-based alloys belong steadily to the most promising materials. Their attractiveness as HS material document a continuous series of review articles reporting one year after another on development and research progress in the field: [9] (2013), [10] (2014), [11, 12] (2015) and [13] (2016). However, the conclusion drawn in the case of magnesium hydride-based HS alloys remains the same: These materials are perspective for HS, but the poor hydrogen sorption kinetics and relative high sorption temperatures are not sufficient as yet for HS applications. One of the possible ways how to improve hydrogen sorption is to find a proper surface catalyst that would facilitate the flux of hydrogen in/out the HS alloy. The catalyst that could provide a sufficiently permeable gate for hydrogen should be thermally stable, oxidation (corrosion) resistant; it should solve hydrogen and enable the hydrogen diffusion time, r_{lim} - preset rate limit).

AAs provide desired features: Very good corrosion resistance that is generally much better than crystalline material of the same chemical composition [14]. This is caused by the absence of chemical and structural inhomogenities that can act as loci of easy corrosion [6, 14]. Rapidly solidified alloys are chemically well

homogeneous and haven not grain and interphase boundaries. At temperatures below the glass transition temperature, the AA can be considered also as a sufficiently stable alloy. Even if partly crystallized (melt-spun nano-alloys, thermally treated AAs), the corrosion resistance remains sufficiently good [15-17]. Moreover, the hydrogen diffusion rate reported in nano-alloys and in AAs is higher than in crystalline counterparts [18-21].

In the present paper, we studied hydrogen absorption in amorphous alloy $Co_{30}Fe_{55}B_{15}$ that seems to be a promising type of possible candidates for catalyst additive to magnesium hydride-based HS alloys.

2. EXPERIMENTAL

2.1. Samples of AA

The samples of $a\text{-}Co_{30}Fe_{55}B_{15}$ were prepared in Department of Metal Physics, Institute of Physics SAS, Slovakia by planar flow casting technique as ribbons of about 10 mm wide and about 30 µm thick. The cast material was used for the measurement as received. The ribbon was cut into small rectangles about 100×5 mm in size. The amount of the cut material for the measurement was about 1 g.

2.2. Alloy Mg₂Ni

The intermetallic Mg_2Ni was prepared by ball milling of Mg (3N8) and Ni (3N6) splinters in ball-mill *Fritsch-Pulverisette6* (10 min milling 450 rpm + 50 min cooling; 20 times repeated; mass ratio of balls to the charge was approximately 60). The milled powder was annealed 360 °C / 20 h / Arand cold compacted into the form of pellets. XRD analysis carried out after the thermal treatment revealed the Mg_2Ni phase only. SEM observation showed that the structure consisted of a mixture of large (typically 100 µm in size) and small (typically 10 µm in size) grains - see **Figure 1a**. After the first hydrogenation, a greater part of the large grains decayed into fragments, which typical size equaled approximately to the size of the smaller grains - see **Figure 1b**.
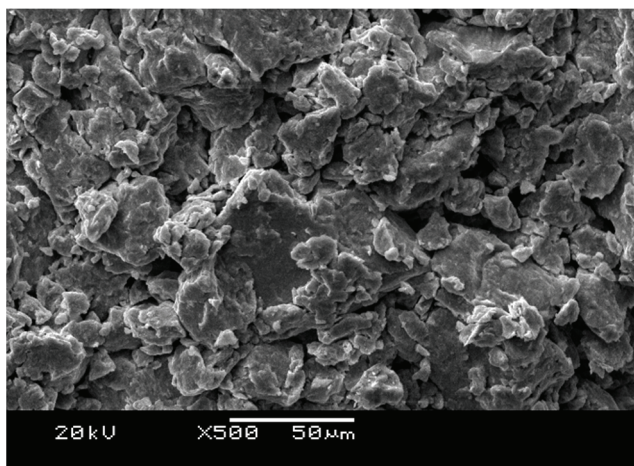

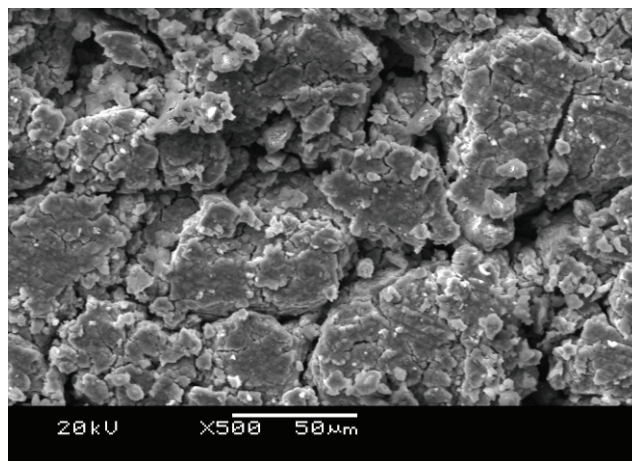| Figure 1a SEM micrograph of Mg₂Ni before hydrogen charging | Figure 1b SEM micrograph of Mg₂Ni after the hydrogen desorption |

Figure 1a SEM micrograph of Mg₂Ni before hydrogen charging

Figure 1b SEM micrograph of Mg₂Ni after the hydrogen desorption

2.3. Measurement

The hydrogen sorption measurements were carried out using the Sieverts-type gas sorption analyzer *PCT-ProSetaram Instrumentation*. The hydrogen pressure p was varied between 10^2 Pa and 6 MPa, test temperatures T were chosen in the interval 150 °C and 350 °C. X-ray diffraction (XRD) was performed using X-ray diffractometer X'Pert Pro MPD (PANAnalytical B.V., Almelo, the Netherlands) using $CoK\alpha_{12}$ radiation

and interpreted by the HighScore Plus software with commercial databases. The structure of samples was checked by SEM JEOL JSM 6460 with EDAX/WEDAX Oxford instrumentation analyzer.

3. RESULTS

3.1. Absorption in $Co_{30}Fe_{55}B_{15}$

Absorption cycling in temperature interval between 150 °C and 350 °C was performed with a single sample, whose weight was about 1 g. From the starting temperature $T = 200$ °C the measurements proceeded at series of test temperatures with the step of 50 °C up to $T = 350$ °C, then the temperature of isothermal cycling decreased by 100 °C down to $T = 150$ °C (**Figure 1**). Each individual isothermal cycling test at given test temperature T consisted of measurement of hydrogen up-take responding the hydrogen doses applied at increasing hydrogen pressure p. Equilibrium hydrogen concentration c_H at temperature T and pressure p was calculated from the hydrogen up-take after the time Δt, needed for the equilibration (after the condition $dc_H/dt < n_{lim}$ was reached; t - time, n_{lim} - preset sorption-rate limit).

Number of cycles n, was chosen so that the stable state was reached (cycling curves did not changed more with increasing n). The first cycles ($n = 1$) are shown in **Figure 2** for all test temperatures (PHC - preliminary hydrogen charged). An example of a complete cycling for $T = 250$ °C and $n = 1,..,6$ is shown in **Figure 3** and a comparison of cycling curves for the stable state (sufficiently high n) are plotted in **Figure 4**. Before the next test temperature T was set, the sample was several times desorbed at the current temperature into evacuated chamber. This desorption procedure was stopped unless the hydrogen pressure increased the rest vacuum pressure (~10 Pa).
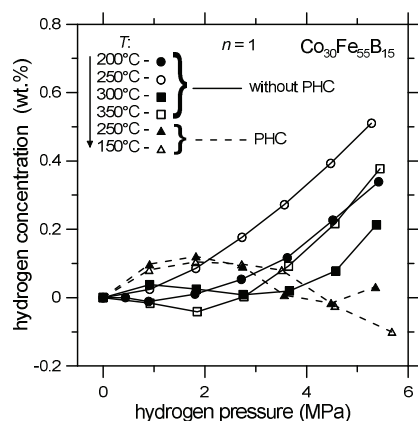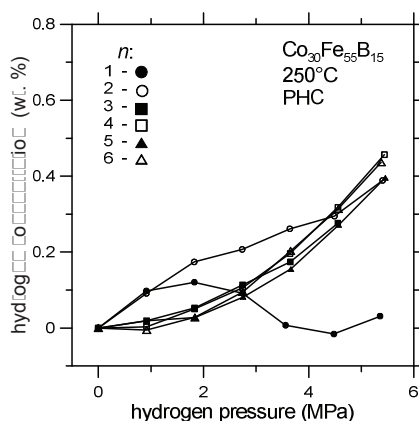

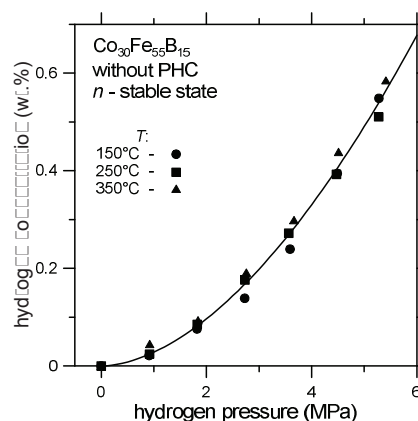**Figure 2** The first cycle   **Figure 3** Successive cycles, 250 °C   **Figure 4** Stable state

XRD patterns shown in **Figure 5** characterize the sample structure in as-received state before the experiment, after the cycling at $T = 200$ °C performed with fresh (second) sample and the structure after the experiment (with maximum temperature $T_{max} = 350$ °C).

3.2 Absorption in Mg_2Ni

For the sake of comparison, hydrogen absorption was measured also in Mg_2Ni intermetallic. The absorption curves are shown in **Figure 6**. The kinetic of hydrogen absorption in the both materials can be compared from kinetic curves in **Figures 7** and **8**, where the examples obtained at the same test temperature $T = 200$ °C are shown.
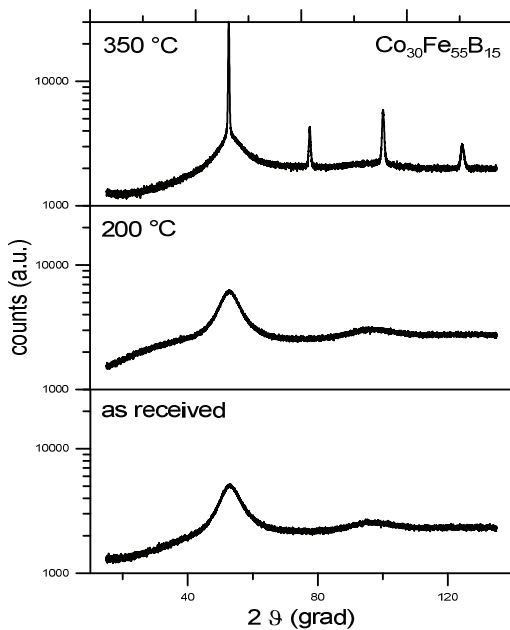
Figure 5 XRD pattern (CoKα₁₂). Structure: As received and after cycling at 200 °C - amorphous, after cycling at T_{max}= 350 °C - amorphous (30-40%)+ bcc solid solution
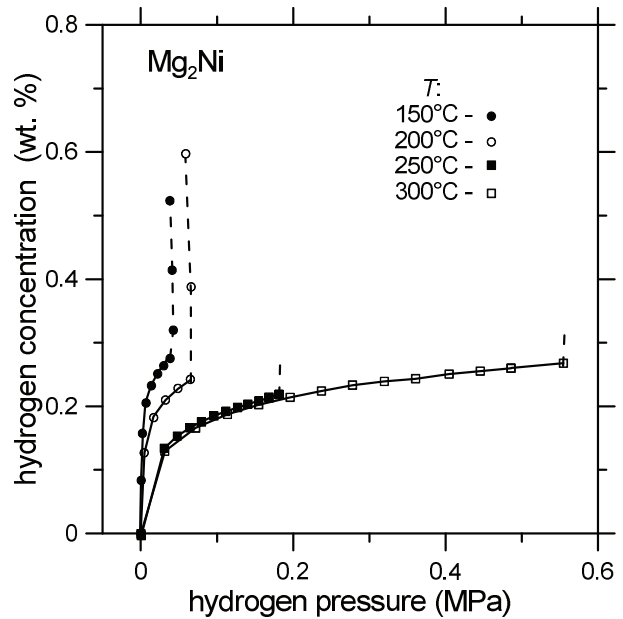

Figure 6 Absorption curves for Mg₂Ni. Stable state (great *n*). Dashed verticals reflect the formation of hydride (phase β)
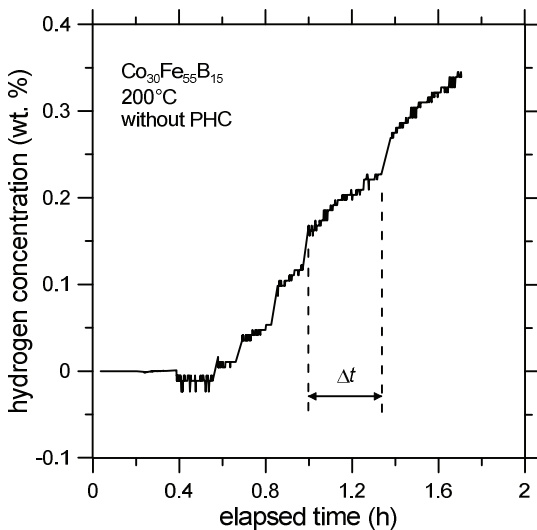

Figure 7 Kinetic curve for Co₃₀Fe₅₅B₁₅. Δ*t* - time to reach the equilibrium
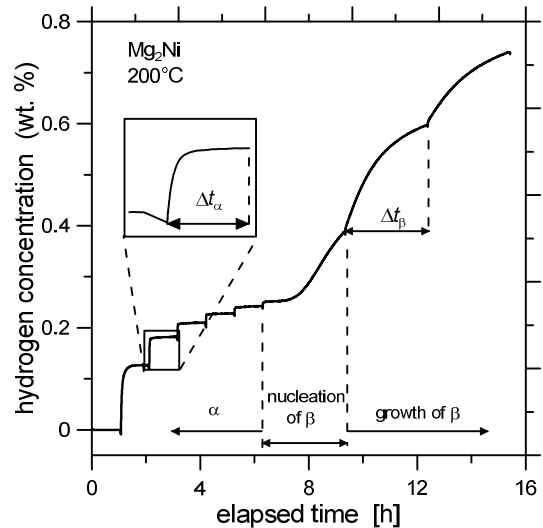

Figure 8 Kinetic curve for Mg₂Ni. Δ*t* - time to reach the equilibrium

4.   DISCUSSION

The arrow in **Figure 2** shows the history of the absorption measurement that started at the test temperature T = 200 °C. It can be seen that the first cycles (n = 1) at all the T's show an inflection in the dependence of hydrogen concentration c_H on hydrogen pressure p. The inflection grows to be less distinct with increasing T and increasing n (see in **Figure 3**). After a few cycles (typically $n \sim 6$), the $c_H = f(p)$ becomes to be without the inflection and to be independent from n (**Figure 3**). It is also obvious from **Figure 4** that c_H does not depend

from T (**Figure 4**) after several cycles: the function f can be well described by relation $c_H = 2089 \cdot p^{1.772}$ (see the curve in **Figure 4**).

The most likely explanation of the inflection in the $c_H = f(p)$ might come from the presence of several (at least two) distinct types of loci that are occupied by hydrogen. The first type of sites is occupied by hydrogen even at room temperature under normal pressure of 0.1 MPa. Hydrogen atoms residing at these sites are expelled easily under the hydrostatic pressure of several MPa (of hydrogen, e.g.). Despite some small amount of hydrogen atoms absorbed at this relatively small pressure p, the net hydrogen up-take in the samples negative. This effect ceases with further cycling and with increasing T and p (**Figures 2 - 4**). When the temperature course is reversed (temperature decrease), certain portion of hydrogen atoms remains in the sites of the first type and despite the de-gassing, the sample behaves as preliminary charged (PHC). Under such condition, the above described effect can be observed again (see measurements conducted at the decreasing temperatures 250 °C and 150 °C in **Figure 2**).

It is worth of noting that the sorption behavior does not change after the exposition the sample to the temperature as high as 350 °C despite the fact that certain portion of amorphous phase crystallizes during such a measurement (**Figure 5**).

Comparing the c_H in Mg_2Ni (**Figure 6**) and $Co_{30}Fe_{55}B_{15}$ (**Figure 2**) at DOI target values of T - up to 150 °C and p 0.1 - 1 MPa [22], it can be seen that c_H is much greater in $Co_{30}Fe_{55}B_{15}$. However, this intermetallic - contrary to alloy $Co_{30}Fe_{55}B_{15}$ - contains a great portion of hydride (β-phase). Hydrogen diffusion in β is very difficult. To illustrate a great difference in hydrogen diffusivity in the two materials, one can compare times Δt needed to approach the equilibrium c_H at target T and p (**Figures 7, 8**). It can be easily obtained that the Δt in $Co_{30}Fe_{55}B_{15}$ is about 40× greater than in Mg_2Ni.

5.   CONCLUSION

In this paper, hydrogen absorption in two materials was compared: Mg_2Ni that is frequently used in Mg hydride-based HS materials and $Co_{30}Fe_{55}B_{15}$, which represent a type of possible alternative candidate materials that might replace the Mg_2Ni. It was found that the equilibrium hydrogen concentration in $Co_{30}Fe_{55}B_{15}$ is slightly lower (about 0.1 wt.% H_2 for $n \leq 2$) than that in Mg_2Ni (about 0.2 wt.% H_2) at the target p and T, but hydrogen sorption kinetics in $Co_{30}Fe_{55}B_{15}$ is much better compared to that in Mg_2Ni at the same conditions. This means that (nano-)particles of $Co_{30}Fe_{55}B_{15}$ could well replace the Mg_2Ni and act as an effective catalyst of hydrogen sorption in Mg hydride-based HS materials.

REFERENCES

[1]   TSENG, J.-Y., CHEN, Y.-T., CHANG, Z. G., et al. Crystallization behavior and thermal analysis of CoFeB thin films. *J. Nanomaterials*, 2015, vol. 2015, Art ID 371894, 6 p.

[2]   KRAUS, L., SOYKA, V., DUHAJ, P., et al. Magnetic properties of nanocrystalline CoFeNbB alloys. *J. Phys. IV France*, 1998, vol. 8, Pr2-95.

[3]   SIMMONS, L. M., GREIG, G., LUCAS, C. A., et al. Time resolved synchrotron x-ray diffraction studies of the crystallization of amorphous Co(80-x)FexB20. *J. Appl. Phys.*, 2014, vol. 116, Art. no. 123514.

[4]   PELLEGREN, J., P., SOKALSKI, V., M. Thickness and interface-dependent crystallization of CoFeB alloy thin films. *IEEE Trans Magnetics*, 2015, vol. 51, no. 11, Art. No. 3400903.

[5]   LEE, S., KIM, K., HWANG, I., et al. Crystallization characteristics of middle CoFeB layer in a double MgO barrier tunnel junction. *Current Appl. Physics*, 2015, vol. 15, no. 1, pp. 38-41.

[6]   INOUE, A., HASHIMOTO, K. (Eds.) *Amorphous and nanocrystalline materials*. Berlin, Heidelberg: Springer 2001, 206 p.

[7]   GRANATA, D., FISHER, E., LOEFFLER, J. F. Effectiveness of hydrogen microalloying in bulk metallic glass design. *Acta Mater.*, 2015, vol. 99, pp. 415-421.

[8]   ZHANG, H.-G., LU, P., WANG, Z.-M., et al. Effect of Mg content on structure, hydrogen storage properties and thermal stability of melt-spun $Mg_x(LaNi_3)_{100-x}$ alloys. *Int. J. Hydrogen Energy*, 2014, vol. 39, pp. 9267-9275.

[9]   HUOT, J., RAVNSBAEK, D. B., ZHANG, J., et al. Mechanochemical synthesis of hydrogen storage materials. *Progress in Mater. Sci.*, 2013, vol. 58, pp. 30-75.

[10]   ZHAO, D.-L., YHANG, Y.-H. Research progress in Mg-based hydrogen storage alloys. *Rare Met.*, 2014, vol. 33 no. 5, pp. 499-510.

[11]   JIA, Y., SUN, C., SHEN, S., et al. Combination of nanosizing and interfacial effect: Future perspective for designing Mg-based nanomaterials for hydrogen storage. *Renewable Sustainable Energy Revs.*, 2015, vol. 44, pp. 289-303.

[12]   ZHANG, Y.-H., JIA, Z.-C., YUAN, Z.-M., et al. Development and application of hydrogen storage. *J. Iron Steel Res. Intern.*, 2015, vol. 22, no. 9, pp. 757-770.

[13]   CRIVELLO, J.-C., DAM, B., DENYS, R. V., et al. Review of magnesium hydride-based materials: development and optimisation. *Appl. Phys A*, 2016, 122:97; DOI 10.1007/s00339-016-9602-0.

[14]   MILLER, M., LIAW, P. (Eds.) *Bulk Metallic Glasses - An Overview*. Oak Ridge, TN: Springer, 2008, 237 p.

[15]   LIAN, T., DAY, D., HAILEY, P., et al. Comparative study on the corrosion resistance of Fe-based amorphous metal, borated stainless steel and Ni-Cr-Mo-Gd. *MRS Proc.,* 2007, vol. 985, pp. 275-280.

[16]   HASHIMOTO, K., KATAGIRI, H., HABAZAKI, H., et al. Extremely corrosion-resistant bulk amorphous alloys. *Materials Sci. Forum*, 2001, vol. 377, pp. 1-8.

[17]   SPASSOV, T., KOSTER, U. Microstructure, microhardness and corrosion behavior of rapidly solidified magnesium based Mg-Ni-(Y,MM) alloys. *Z. Metallkunde,* 2000, vol. 91, no. 8, pp.675-679.

[18]   SPASSOV, T., KOSTER, U. Hydrogenation of amorphous and nanocrystalline Mg-based alloys. *J. Alloys Compd.*, 1999, vol. 287, no. 1-2, pp. 243-250.

[19]   APIH, T., JASTROW, L., LYUBENOVA, L., et al. Hydrogen diffusion in Zr-Cu-Ni-Al metallic glasses. *Mater. Res. Soc. Sym. Proc.*, 2004, vol. 801, pp. 107-112.

[20]   ZHANG, Y., HU, F., LIU, Z., et al. Investigation of electrochemical hydrogen storage kinetics of melt spun nanocrystalline and amorphous Mg_2Ni-type alloy. *Rare Metal Mater. Eng.*, 2012, vol. 41, no. 4. pp. 565-569.

[21]   WU, Y., LOTOTSKY, M., V., SOLBERG, J. K. Microstructure and novel hydrogen storage properties of melt-spun Mg-Ni-Mm alloys. *J. Alloys Compd.,* 2009, vol. 477, no. 1-2, pp. 262-266.

[22]   HIRSCHER, M. (Ed) *Handbook of Hydrogen Storage*. Weinheim: Wiley-VCH Verlag GmbH & Co. KGaA, 353 p.